DARK MATTER AND SHOCKED PANCAKES

J.R. Bond[1,2], J. Centrella[3], A.S. Szalay[4,1], and J.R. Wilson[5]

[1] Institute of Astronomy, Cambridge University
[2] Institute of Theoretical Physics, Stanford University
[3] Astronomy Department, University of Illinois
[4] Department of Atomic Physics, Eötvös University, Budapest
[5] Lawrence Livermore Laboratories.

We classify massive stable collisionless relics of the Big Bang into three categories of dark matter: hot, with damping mass about supercluster scale; warm, with damping mass of galactic or cluster scale; and cold, with negligible damping. The first objects that form in universes dominated by hot and warm relics are pancakes. Coupled one-dimensional N-body and Eulerian hydrodynamical simulations follow the nonlinear evolution of pancakes, the separation of baryons from dark matter via shock formation and the evolution of the shocked gas by conduction as well as by cooling. We sketch a simple analytic theory based upon the uniformity of pressure over the shocked region which accurately describes our numerical results. Only $\sim$10-20% of the gas cools sufficiently to fragment on sub-galactic scales in neutrino-dominated (hot relic) theories. Cooling is efficient for warm relics. In all cases, the typical fragment size is $\sim 10^9$-10^{10} $M_\odot$.

1. CLASSIFICATION OF DARK MATTER CANDIDATES

Stable collisionless relics of the Big Bang are perhaps the most attractive candidates for the dark matter. Bond and Szalay (1983) have classified the possibilities into three basic types defined by their background velocity dispersion: relics may be hot, warm, or cold. The canonical example of a hot relic is a massive neutrino, with velocity dispersion $6(m_\nu/30\mathrm{eV})^{-1}(1+z)$ km s^{-1}.

J. Audouze and J. Tran Thanh Van (eds.),

However, any particle which is massive, stable and decouples when relativistic at an epoch when the temperature of the universe was $\lesssim T_{qh} \sim 200$ MeV is a hot particle. Any particle which decouples at a temperature above T_{qh} is warm, with velocity dispersion $0.085(100/g(T_d))^{1/3}(1\ \mathrm{keV}/m_x)$ km s^{-1}. Here, we call our hypothetical collisionless relic X, and m_x is its mass; $g(T_d)$ is the effective number of degrees of freedom at the X-decoupling temperature, T_d. The quark-hadron phase transition temperature, T_{qh}, is the approximate decoupling boundary between warm and hot since above T_{qh} the number of relativistic species present is large due to all the liberated quark-antiquark pairs. At the neutrino decoupling temperature, $T_d \sim 1$ MeV, g is only 10.75, whereas $g \simeq 60$ just above T_{qh}. Near electroweak unification at $\sim$100 GeV, $g \sim 100$ in the minimal Weinberg-Salam SU(2) $\otimes$ U(1) $\otimes$ SU(3) theory. Near grand unification energies, $\sim 10^{15}$ GeV, $g \sim 160$ in the minimal Georgi-Glashow (1974) SU(5) theory. Supersymmetric theories increase g by only a factor of about two.

The relationship between the density parameter of relativistic decouplers and their mass is: $\Omega_x = 1.1\ h^{-2}\ (100/g(T_d))\ m_x/1$ keV, where h is Hubble's constant in units of 100 km s^{-1} Mpc^{-1}. For $g = 10.75$, we get the usual $20\text{-}10^2$ eV mass meeded for one species of massive neutrino to close the universe. The variation corresponds to the range $h = 0.5$ to 1. For $T_d > T_{qh}$, and for minimal theories, $m_x \cong 2\times10^2 - 2\times10^3$ eV is the mass required for $\Omega = 1$. This mass could be much larger if: (1) there is no large plateau in g(T) - i.e. no desert; (2) significant entropy generation occurs after T_d - Ω_x scales inversely with the entropy amplification factor. The first option could be restricted since the number of stable relativistic neutrino species at the time of primordial helium generation cannot be much greater than three to avoid overproduction (Schwartzman 1969, Olive et al. 1981); this could translate into a constraint on the number of leptoquark families. The second option suffers from constraints on the allowable entropy generation after baryon synthesis.

Hot particles have a damping scale arising from the constructive effects of gravitational attraction on large scales and the destructive effects of their random velocity on small scales: $M_d \cong 3.4\ m_p^3/m_x^2$ (Bond, Efstathiou and Silk 1980), where $m_p = 1.22 \times 10^{22}$ MeV is the Planck mass; this is of supercluster scale. Warm particles damp below the scale

$$M_d \cong 0.11\ (m_p^3/m_x^2)\ (100/g(T_d))^{4/3} \qquad (1)$$

(Bond, Szalay and Turner 1982, Bond and Szalay 1983), which is either the scale of galaxies or of clusters depending upon h. If m_x is very large, due to either (1) or (2), then the damping scale can be very small, and the particles are effectively cold. Indeed, we define cold particles to be those with almost no

velocity dispersion, and which thus have $M_d \simeq 0$. Collisionless relics which decouple when they are nonrelativistic are examples. Preskill, Wise and Wilczek (1982) have recently pointed out that oscillations of "classical" fields, i.e. of boson vacuum expectation values, can lead to a large time-averaged energy density, as well as to a rapidly fluctuating part. They claim that spatial fluctuations in the field have energy density growth identical to that of nonrelativistic decouplers.

The canonical hot particle is the massive neutrino. Another candidate is the Majoran, a goldstone boson whose raison d'être is to generate neutrino masses via spontaneous symmetry breaking (Georgi, Glashow and Nussinov 1981, Gelmin, Nussinov and Roncadelli 1982). All background $\nu\bar{\nu}$'s would annihilate into a sea of Majorans - the temperature of which would be higher than that of the background photons. If they are massive, then $m \lesssim 10$ eV is required in order to have $\Omega \lesssim 1$. This implies uncomfortably large damping masses and, as we shall see, very little gas cooling in a Majoran-dominated universe. Suggestions for warm relics have included the gravitinos and photinos of supersymmetric theories, and right-handed neutrinos. Any of these could also decouple when non-relativistic, and thus be cold. Heavy neutral leptons of the sort discussed by Lee and Weinberg (1977), primordial black holes, and monopoles are other cold relic candidates. If strings form in phase transitions in the very early universe, and if they primarily exist as loops of subgalactic dimensions (Kibble 1983), galaxy formation in string-dominated universes will effectively follow the cold scenario. The model for classical field oscillation is provided by the axion (Preskill, Wise and Wilczek 1982).

In all cases in which relics form the dark matter, a remarkable coincidence is required - namely that Ω_x and Ω_B are not too dissimilar. We know that Ω_B cannot be too small, or else cooling on any scales would have been too inefficient. This is an anthropic argument which rules out extreme variations of Ω_B. If $\Omega \simeq 1$ is required as a consequence of inflation (or simplicity), and m_x is given by the particle physics, then H_o would be adjusted so that the $\Omega_x \sim m_x h^{-2}$ relation is enforced for relativistic decouplers; the coincidence $\Omega_x \sim \Omega_B$ implies $m_x \sim m_N s^{-1}$, where $s \sim 10^9$ is the entropy per baryon and m_N is the nucleon mass. In a simple model of baryon generation, this becomes $m_x \sim m_N m_p m_{VB}^{-1} \alpha_{GUT} \varepsilon_{CP}$, where m_{VB} is the mass of the intermediate vector boson responsible for baryon generation, α_{GUT} is the fine structure constant at unification energies, and ε_{CP} is a CP-violating parameter. Why should such quantities be interrelated in this manner? The case of nonrelativistic decouplers requires perhaps an even more stringent restriction upon the particle physics, namely that the freeze-out temperatures for the reactions which create X's must be - within some narrow range - a

prescribed fraction of m_x ($15 \lesssim m_x/T_{fx} \lesssim 50$ for 1 GeV $\lesssim m_x \lesssim 10^{15}$ GeV).

2. COOLING SCALE AND PANCAKES

We have seen that the $m_p^3\ m_x^{-2}$ damping scale applies for hot and warm particles; compare this with the mass scale of stars which is set by the combination $m_p^3\ m_N^{-2} = 1.9\ M_\odot$. Another scale at high mass enters into the determination of the fluctuation spectrum: the horizon mass at equipartition between relativistic and nonrelativistic constituents, which occurs at $z_{eq} = 25000\ \Omega h^2$ when the photon temperature is $T_{\gamma eq} = 5.8\ \Omega h^2$ eV:

$$M_{Heq} = 0.2\ m_p^3\ T_{\gamma eq}^{-2} \approx 10^{16}\ (\Omega h^2)^{-2}\ M_\odot$$

An initially scale-free density spectrum evolves in the linear phase to one in which there is a sharp damping cutoff at masses smaller than M_d, a strong flattening between M_d and M_{Heq} which then matches onto the original spectral shape above M_{Heq} (Peebles 1982, Bond, Szalay and Turner 1982, Bond and Szalay 1983). It has been conventional to associate the appearance of voids and strings in the galaxy distribution with a large damping cutoff. An important unresolved issue is whether the shoulder below M_{Heq} is sufficient to generate such structure. In any case, for warm and hot particles, the first structures to become nonlinear will be on the scale M_d, will collapse preferentially along one axis, becoming highly asymmetric, and result in shock formation in the central regions (Zeldovich 1970, Sunyaev and Zeldovich 1972). The first structures to collapse in the cold scenario may also be asymmetric and lead to shocks; however, instead of a smooth collective inflow, the shocks may be more localized, arising from cloud-cloud collisions.

Binney (1977), Rees and Ostriker (1977) and Silk (1977) have demonstrated how galaxy masses may be related to a cooling scale. It is instructive to go through this exercise to demonstrate what must be done to get cooling in larger structures - from which galaxies ultimately arise. The Rees and Ostriker (1977) development yields

$$M_{cool} \sim \frac{m_p^3}{m_N^2} \frac{\alpha^5 m_p}{(m_e m_N)^{\frac{1}{2}}} \frac{\Omega_B}{\Omega} \sim 2\times10^{10} \frac{\Omega_B}{\Omega} \cdot M_\odot \ . \qquad (2)$$

The ingredients which go into obtaining this scale are as follows. A virialized homogeneous sphere cools via bremsstrahlung faster than free-fall if its temperature satisfies:

$$T/m_e < M\ m_p^{-3}\ m_N^2\ (m_N m_e)^{\frac{1}{2}}\ m_p^{-1}\ \alpha^{-3}\ \Omega\ \Omega_B^{-1} \ .$$

However, the temperature $T \sim M^{2/3}(1+z_t)$ depends not only upon the mass, but also upon the epoch of turn-around, z_t. Indeed, if z_t is too large, Compton cooling should replace bremsstrahlung. In any case, stability can never be regained if T falls in the helium-hydrogen recombination cooling regime. Since the ionization energy of helium is $2\alpha^2 m_e$, and the characteristic temperature for helium recombination is some fraction of this, we obtain the scale M_{cool}. There are 3 ways to increase M_{cool}: (1) raise z_t into the Compton cooling epoch; (2) utilize central condensation so that T can be lower in the central regions since the matter has less far to fall before shocking; (3) stretch the sphere into an oblate configuration so again the gravitational acceleration is less. Effects (2) and (3) operate in pancakes; z_t is constrained by limits on the temperature fluctuations in the microwave background, hence (1) cannot be pushed too far.

3. PANCAKE SHOCK CALCULATIONS

This work is described more fully in Bond, Centrella, Szalay and Wilson (1983), hereafter BCSW. Here, we outline the methods and give the main results. A pancake collapse similar to our runs without conduction has recently been computed by Shapiro, Struck-Marcell and Melott (1983).

3.1 Initial Conditions and the Zeldovich Solution.

We let $\underset{\sim}{\xi}$ and $\underset{\sim}{x}$ denote comoving Lagrangian and Eulerian spatial variables. We ignore the effects of random velocity dispersions of the collisionless relics since these redshift away as the universe expands, and are small relative to the gravitationally-induced velocities at the time of pancaking (Bond, Szalay and White 1983). For such cold initial conditions, the Zeldovich (1970) solution describes the deviations of the particle positions at time t from their initial values by

$$x(\xi,t) = \xi - b(t)\,\eta(\xi)$$

where $b = (1+z)^{-1}$ in the Ω=1 models we are most concerned with; and $\eta(\xi) = (kb_c)^{-1} \sin(k\xi)$ for a single plane wave of comoving wavenumber k and wavelength $L \equiv 2\pi k^{-1}$. A caustic forms when x=0, at $b=b_c$. This formula is exact in the linear regime, and in one-dimension until caustic formation. It also describes the early nonlinear phases of 3-dimensional evolution rather well.

The distribution of the principal eigenvalues, λ_i, of the (anti-) strain tensor $(\partial\eta_i/\partial\xi_j)$ describes the 3-dimensional patterns which first appear in the nonlinear evolution of a density fluctuation spectrum with a damping cutoff. The overdensity is related to these eigenvalues by

$$1 + \delta = (1-b\lambda_1)^{-1} (1-b\lambda_2)^{-1} (1-b\lambda_3)^{-1} . \qquad (3)$$

The principal axes, 1,2,3, are always ordered so that $\lambda_1 \geqq \lambda_2 \geqq \lambda_3$. Therefore, by definition, collapse is most rapid along the 1-axis; and caustics, where $\delta \to \infty$, occur at λ_1-maxima. The surfaces of λ_1-maxima are generally curved, with curvature at most of order the damping scale. Different surfaces intersect at points of degeneracy of the 1 and 2-axes, where $\lambda_1 = \lambda_2$. More extreme point-like configurations form where all 3 axes are degenerate. These topological structures are catalogued by Arnold, Shandarin and Zeldovich (1982). In the neighbourhood of every λ_1-maxima surface, the flows are essentially one-dimensional: we expect our 1D simulations to describe the post-caustic evolution of these regions rather well. Directions 2 and 3 may continue undergoing transverse expansion which differs little from the Hubble expansion initially. However, within a few Hubble times of the collapse redshift, transverse flows toward the 1-2 degeneracy lines (strings) may become important. To model this in our 1-D calculations, we utilize an anisotropic expansion factor, $a_2(t) = a(t)(1-b(t)\lambda_2)$, where λ_2 is taken to be constant. This approximation may be quite reasonable since BCSW demonstrate that the tidal force toward strings dominates the pressure gradients opposing such motion, so dark matter and shocked gas should flow toward the strings together, following the Zeldovich solution.

3.2 Evolution Equations.

Neutrinos are followed by direct N-body simulation of their equations of motion: $dva^2/dt = -\nabla\phi$, where $v=dx/dt$ is the comoving peculiar velocity. The gravitational field equations reduce - for these nonrelativistic particles - to Poissons equation, except that the source is the overdensity relative to the background. This couples the N-body code to the gas dynamical code - which utilizes Eulerian hydrodynamics in comoving space. We solve transport equations for the following quantities: (1) Baryon number. (2) Momentum - artificial viscosity is used to treat shocks. (3) Matter energy, including ionic and electronic contributions. Artificial viscosity provides the shock heating. Energy losses arise from bremsstrahlung, Compton cooling, and He and H recombination cooling. Flux-limited conduction is included: transfer primarily occurs via electron-electron collisions, although ion-ion collisions are also incorporated. (4) Ion energy. This transport equation includes ion-ion conduction, and a term describing the relaxation of the ionic temperature towards the electron temperature via ion-electron collisions. It is the ions which are shock-heated and the electrons which cool. The ion and electron temperatures can therefore differ - especially near the shock front. The equation of state is that of an ideal gas with ionization fraction determined by the balance of collisional ionization ($eH \to epe$) with recombination ($ep \to H\gamma$). We do not

explicitly calculate the He ionization fraction; it is, however, included in the cooling rate. Complications arise since the pancakes are generally optically thick in their central regions to Ly α and to radiation above the Ly edge. Still, lower energy radiation escapes, allowing continual rapid cooling.

3.3 Pancake Timescales.

Some of the timescales of relevance to the shock problem are plotted as a function of temperature in Fig. 1 for a specific choice of the baryon density - which corresponds to an overdensity of 10^2 above that of the background gas.

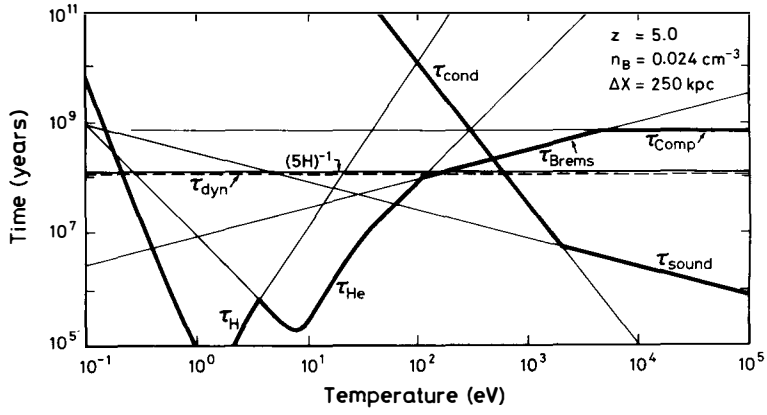

Figure 1. Characteristic timescales under typical pancake conditions.

The bremsstrahlung and He and H recombination cooling times scale with density as n_B^{-1}, but for given n_B are redshift-independent. Compton cooling is n_B-independent, but varies as $(1+z)^{-4}$. One does not have to go to very large redshift before Compton cooling completely overtakes bremsstrahlung. The conduction timescale across a region of size Δx of uniform density is also plotted; the scaling is $\tau_{cond} \sim n_B (\Delta x)^2 (1+z)^{-2}$. This illustrates that conduction is primarily important in the outer shocked regions. When the sound crossing time across Δx, $\tau_s \sim (1+z)^{-1} \Delta x$, exceeds τ_{cond}, we are in the flux-limited transport regime. These cooling and conduction timescales are compared with the dynamical timescale for the collapsing baryon layer, or with $(5H)^{-1} \sim (1+z)^{-3/2}$- the latter choice is better. (See §3.5).

The major point of Fig. 1 is that once T falls below 100 eV, cooling is very rapid.

3.4 Shock Evolution.

We began our calculations in the linear regime, $\delta<<1$. The initial phase of the collapse just demonstrates the validity of the Zeldovich solution - even for the gas, which has a small pressure. However, near the redshift of caustic formation, z_c - the collapse redshift - the central density rises rapidly (Eq.3), and the gas pressure builds up due to the adiabatic compression. The shock forms approximately at the point where the incoming ram pressure equals this gas pressure (Sunyaev and Zeldovich 1972), i.e. near the sonic point. The collisionless relics begin to separate from the gas after this. In Fig. 2, overdensities of baryons and neutrinos are given as a function of comoving position for a pancake of wavelength 25 Mpc which caustics at $z_c=5$. The universe has $\Omega=1$, $\Omega_B=0.091$ and h=1. The neutrinos form density spikes at the edges of the well known phase space spirals which appear in 1D simulations (See, e.g. Bond, Szalay and White 1983). The gas is confined by the ram pressure, much of it to a region smaller than 10 kpc. The spread in neutrinos is more than an order of magnitude greater at these times.

The temperature profile evolution for the 25 Mpc pancake is shown in Fig. 3. Conduction clearly transports energy from the hot exterior inward, thereby flattening the temperature gradient. The profiles drop precipitously toward 1 eV and hydrogen recombination below $T \sim 100$ eV. By z=4.8, $\sim$9% of the gas has cooled below this temperature; by z=3, 11% has cooled with conduction, 14% without. It takes conduction time to operate. This is especially evident in Fig. 4: a 54 Mpc pancake begins with only $\sim$4% of the gas cold; an inward-eating conduction front breaks through the center by z=3.8, resulting in essentially a flat profile by z=3. For small wavelength runs, the temperatures achieved are lower, conduction is relatively unimportant, and a large fraction of the gas cools.

Transverse compression results in adiabatic heating of the outer regions, but very rapid cooling of the inner ones. The boundary between the two regimes occurs at a mass fraction q=0.15 for our standard L=25 Mpc model, hence does not result in a significant increase in cooling fraction.

3.5 Semi-analytic Shocks.

The major feature of our numerical runs is that *the pressure is constant behind the front, and is equal in magnitude to the ram pressure*. The ram pressure can be determined from the Zeldovich solution exterior to the shocked region (Sunyaev and

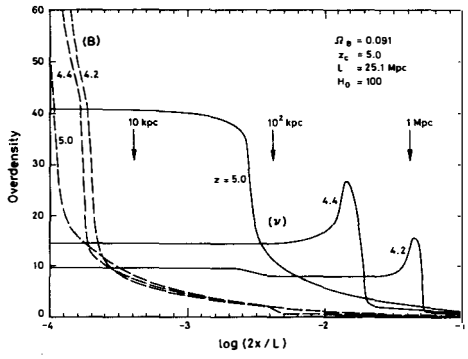

Figure 2. Overdensity of baryons, B, and of neutrinos, ν, - relative to their backgrounds - against comoving position.

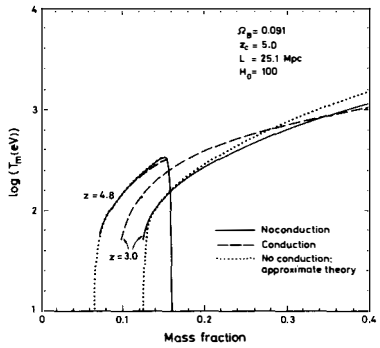

Figure 3. Temperature profile against gas fraction.

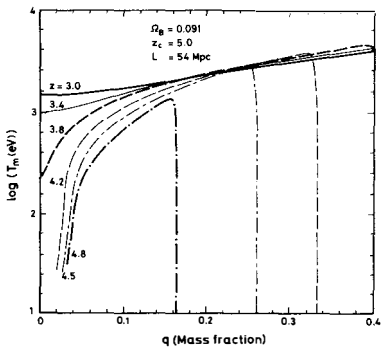

Figure 4. Temperature profile of 54 Mpc - pancake shows the central breakthrough of the conduction front.

Zeldovich 1972):

$$p(q,z) \approx P_{RAM} \approx 1.9\times10^{-14}(1+z)^4(hL_{10})^2\Omega_B h^2 f(z) \text{erg cm}^{-3} , \quad (4)$$

for $q < q_s(z)$, where L_{10} is the wavelength in 10 Mpc units and $q_s(z)$ is the shocked mass fraction at z. The redshift-dependent function f(z) depends upon the initial profile, the transverse motion, and the value of Ω. For $\lambda_2=\lambda_3=0$, f differs greatly from unity only when q_s is large (BCSW): the $(1+z)^4$ term dominates the p_{RAM}-evolution.

In conjunction with Eq.(4), the Rankine-Hugoniot relations for conservation of baryon number, momentum and energy across the front - with incoming quantities determined by the Zeldovich solution - yield a complete theory of the shocked region. For example, the temperature just behind the front is approximately

$$T(q, z_s(q)) \cong 430\ (1+z_s)\ q^2\ (h\ L_{10})^2\ \text{eV} \quad (5)$$

The neglect of pressure gradients, and also of gravitational potential gradients, which is justified by the ram confinement, reduces our full equations to a single one for T:

$$\left(\frac{\partial \ln T}{\partial \ln a}\right)_q \equiv -\nu(a,T,q) \equiv -\nu_s - \nu_c , \quad (6)$$

$$\nu_s \equiv -\frac{2}{5}\frac{d \ln P_{RAM}(a)}{d \ln a} , \quad (7)$$

$$\nu_c \equiv (5H(a)\ \tau_{cool}(a,T))^{-1} . \quad (8)$$

For simplicity, we have not included conduction, which would turn Eq.(6) from an ODE into a PDE. Near $a_s(q) = (1+z_s(q))^{-1}$, when the shock is at gas fraction q, $T \propto T_s(a_s/a)^\nu$, hence we term ν the cooling power. The initial condition for Eq.(6) is Eq.(5). For adiabatic cooling, only ν_s is non-zero; using (4), we have $\nu_s \sim 8/5$ for $f\simeq1$. Eq.(6) is easily numerically integrated with all correction factors included. The agreement with our full numerical no-conduction runs is very good, as Fig. 3 demonstrates.

4. COOLING FRACTIONS AND FRAGMENT SIZES

In Fig. 5, we plot the fraction of gas which has cooled below 100 eV by z=3 for z_c=5 collapses, q_c. Below 100 eV, cooling down to 1 eV occurs rapidly; 100 eV is also the virial temperature for

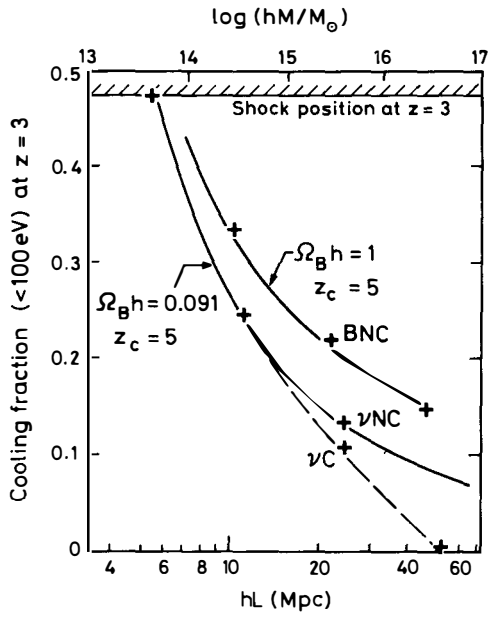

Figure 5. Fraction of cold gas as a function of pancake scale. Crosses are numerical results: νC and νNC are neutrino-dominated universes with and without conduction, for which h=1; BNC are pure baryon universes with no conduction included. The solid and dashed curves are analytic results; the latter includes conduction effects, the former does not.

a typical galactic halo. The solid line gives the solution to Eq.(6) with only bremsstrahlung cooling included, and transverse Hubble expansion assumed.

$$q_c = A(hL_{10})^{-1} \left(1 + B\,\Omega_B\, h\, (hL_{10})^2\right)^{1/3}, \qquad (9)$$

$$A = 0.27 \left(\frac{1+z_c}{6}\right)^{3/10} \left(\frac{4}{1+z}\right)^{4/5},$$

$$B = 1.0 \left(\frac{1+z_c}{5}\right)^{1/10} \left(\frac{1+z}{4}\right)^{12/5} \frac{\{1-(\frac{1+z}{1+z_c})^{1/10}\}}{0.04}.$$

A and B are only weakly dependent upon z_c, assuming we are not in the Compton cooling regime, but are relatively sensitive to z. In BCSW, we also give an approximate solution with conduction included (dashed curve). Both expressions agree well with our full runs.

The comoving size of the cooled region can be computed from the cooled fraction:

$$d \cong 4.7\ h^{-1}\ q_c\ (hL_{10})^{-1}\ \text{kpc}\ ,$$

which turns out to be much smaller than the usual 3-dimensional Jeans length. It is more appropriate to consider the longitudinal dimension of the fragmenting region fixed at d; the transverse dimension of the most rapidly growing perturbation is then given by the Sunyaev-Zeldovich length:

$$L_{SZ} \cong 77\ (1+z)^{-1}\ (q_c L_{10})^{-1}\ \text{kpc}.$$

The fragments are thus initially extremely elongated, but can rapidly undergo transverse collapse at the freefall rate due to the efficiency of cooling. The mass of the fragments is

$$M_{SZ} \approx 5 \times 10^8\ (\Omega_B h)^{-1}\ (hL_{10} q_c)^{-1}\ M_\odot\ . \qquad (10)$$

According to Eq.(9), M_{SZ} is only weakly dependent upon the pancake mass; for $\Omega_B \sim 0.1$, we have $\sim 10^{10}\ M_\odot$ representing the typical fragment scale.

5. DISCUSSION

If we assume the density fluctuations are initially adiabatic, the nature of the dark matter determines how the large scale structure first arises. If cold relics dominate, the theory is a variant of the hierarchical clustering picture developed by White and Rees (1978) for the isothermal picture with dark matter. Peebles (1984) and Primack (1984) discuss the many positive aspects of this picture in this volume. However, it is difficult to see how (1) superclusters and large voids arise, (2) Ω can be one - if indeed it is one. If warm relics dominate, cooling is no problem, but again (1) and (2) do not come naturally. Further, dwarf irregulars and ellipticals would have to arise via fragmentation in the warm scenario, and if M_d is of cluster scale, so would all galaxies.

In neutrino-dominated models, (1) and (2) could naturally follow. On the other hand, building a theory with $\sim$90% of the gas too hot to immediately condense on galaxies could be a problem. The X-ray emitting gas in rich clusters cannot have a mass much larger than $\sim$2 times that in the galaxies of the clusters (Ku et al. 1982). However, since rich clusters may arise at the points of 3-fold eigenvalue degeneracy, and their gas has $T \sim 7$ keV,

which is significantly higher than that of pancake gas, we should not identify the two sorts of hot gas. Intergalactic gas with $T > 10$ eV and one-tenth the critical density cannot be ruled out (Sherman 1982). Indeed, it may be desirable to have most of the baryons unclustered on galactic scales, since there is apparently a gap between the baryon density required at the primordial nucleosynthesis epoch to generate consistent light element abundances (Gry 1984, Schramm 1984) and that inferred from luminous matter. Thus, the neutrino theory may well survive this cooling problem.

REFERENCES

Arnold, V.I., Shandarin, S.F. and Zeldovich, Ya.B. 1982, Geophys. Astrophys. Fluid Dynamics 20, 111.

Binney, J. 1977, Ap. J. 215, 483.

Bond, J.R., Efstathiou, G. and Silk, J. 1980, Phys. Rev. Lett. 45, 1980.

Bond, J.R. and Szalay, A.S. 1983, Ap. J., in press.

Bond, J.R., Szalay, A.S. and Turner, M.S. 1982, Phys. Rev. Lett. 48, 1636.

Bond, J.R., Centrella, J., Szalay, A.S. and Wilson, J.R. 1983, M.N.R.A.S., to be published.

Bond, J.R., Szalay, A.S. and White, S.D.M. 1983, Nature 301, 584.

Gelmini, G.B., Nussinov, S. and Roncadelli, M. 1982, preprint MPI-PAE/Pth 37182.

Georgi, H. and Glashow, S.L. 1974, Phys. Rev. Lett. 32, 438.

Georgi, H., Glashow, S.L. and Nussinov, S. 1981, Nuc. Phys. B 193, 297.

Gry, C. et al. 1984, this volume, p. 279.

Kibble, T.W. 1983, private communication.

Ku, W.H.M. et al. 1982, M.N.R.A.S. 202.

Lee, B.W. and Weinberg, S. 1977, Phys. Rev. Lett. 39, 165.

Olive, K.A., Schramm, D.N., Steigman, G., Turner, M.S. and Yang, J. 1981, Ap. J. 246, 557.

Peebles, P.J.E. 1982, Ap. J. 258, 415.

Peebles, P.J.E. 1984, this volume, p. 185.

Preskill, J., Wise, M.B. and Wilczek, F. 1982, Harvard preprint HUTP-82/A048.

Primack, J.R. and Blumenthal, G.R. 1984, this volume, p. 163

Rees, M.J. and Ostriker, J. 1977, M.N.R.A.S. 179, 541.

Schramm, D.N. and Freese, K. 1984, this volume, p. 197.

Schwartzman, V.F. 1969, Sov. Phys. JETP Lett. 9, 184.

Shapiro, P.R., Struck-Marcell, C. and Melott, A.L. 1983, preprint.

Sherman, R.D. 1982, Ap. J. 256, 370.

Silk, J. 1977, Ap. J. 211, 638.

Sunyaev, R.A. and Zeldovich, Ya.B. 1972, Astron. Astrophys. 20, 189.

Zeldovich, Ya.B. 1970, Astron. Astrophys. 5, 84.